# Electrochemically- and Photoinduced Infrared Bands in PPV: A Comparative Study

Helmut Neugebauer[a], Shankaran Srinivasan[a], Stefan Tasch[b], Günther Leising[b] and N. Serdar Sariciftci[a]

[a]Physical Chemistry, University of Linz, Altenbergerstraße 69, A-4040 Linz, Austria
[b]Institute of Solid State Physics, Technical University of Graz, Petersgasse 16, A-8010 Graz, Austria

## ABSTRACT

Results of *in situ* Fourier transform infrared attenuated total reflection (FTIR-ATR) spectroscopy during electrochemical oxidation processes (electrochemically induced doping) as well as by photoinduced infrared absorption spectroscopy (photoinduced doping) of polyparaphenylenevinylene (PPV) are presented. Infrared active vibrational (IRAV) bands in the lower energy part of the infrared spectrum and infrared absorption due to electronic transitions at higher energies are observed and compared. The electrochemical doping of PPV occurs in two potential regions. In the "low doping" region, the difference spectra obtained by *in situ* FTIR-ATR spectroscopy are similar to spectra obtained by chemical doping. In the "high doping" region, the spectral behavior is different to the "low doping" region and shows a higher similarity to the photoinduced absorption spectrum.

**Keywords:** In situ spectroscopy, spectroelectrochemistry, FTIR-ATR spectroscopy, electrochemical doping, photoinduced doping, photoinduced absorption spectroscopy, polyparaphenylenevinylene (PPV), infrared active vibration (IRAV) bands

## INTRODUCTION

Vibrational spectroscopy is a valuable tool to study the properties of conjugated polymers on a molecular level and to obtain a detailed knowledge of molecular structures and electronic configurations of these highly interesting substances[1]. Due to the existence of a network of delocalized π-electrons, the spectra of conjugated polymers show unusual features, especially in the doped, conducting form and in the photoexcited state. Upon doping, new infrared active vibrational (IRAV) bands appear in the spectrum, due to the formation of self-localized charged excitations (polarons or bipolarons), which lead to structural distortions of the polymer lattice in the vicinity of the charge breaking the local symmetry[2]. The formation of the charged excitations can be obtained either by chemical doping, by electrochemical doping or by photoexcitation. Chemical and electrochemical doping leads to additional structural influences of the incorporated dopant counter ions in the polymer matrix, which are not present using photoexcitation. Differences in the IRAV spectra of doped and photoexcited conjugated polymers are therefore expected. Theoretical calculations on frequencies and absorption intensities of IRAV bands (considering also Raman spectroscopy) and their connection to relevant physical characteristics have been published by several groups[3,4].

Electrochemical doping of conjugated polymers represents a favorable way compared with chemical doping, since the doping degree can be controlled easily by adjusting electrochemical parameters (e.g. electrode potential). The simultaneous application of advanced spectroelectrochemical techniques in the infrared spectral range allows the measurement of spectral features *in situ*, i.e. in contact with the electrolyte solution and under applied potential[5-7]. A direct correlation of spectral effects with electrochemical parameters and with the degree of doping can be obtained.

Polyparaphenylenevinylene (PPV) is an interesting polyconjugated material[8], which attracted major scientific attention for its special optical properties[9,10] and high electrical conductivity upon doping[11,12]. PPV can be obtained via its precursor, which is soluble in common organic solvents, thereby offering flexibility in processing. The doping process can be performed electrochemically[13]. The conversion of PPV into the doped conducting form by electrochemical oxidation appears in two steps, a fully reversible first oxidation step at lower electrode potentials and a partly irreversible process at higher electrode potentials[14].

In the present paper, we present for the first time *in situ* investigations on the electrochemical doping of PPV using Fourier transform attenuated total reflection (FTIR-ATR) spectroscopy, with special emphasis to differences in the "low doping" region (up to 1050 mV vs. SCE) compared to the "high doping" region (above 1050 mV vs. SCE). Furthermore, the electrochemically induced IRAV spectra are compared with spectra obtained by photoinduced absorption spectroscopy.

## EXPERIMENTAL

Thin films of PPV were prepared via pyrolysis of a soluble precursor polymer[15], which was drop cast on the IR substrate. For the spectroelectrochemical investigations, the substrate was a germanium reflection element (50 x 20 x 3 mm), for the photoinduced absorption measurements the film was prepared on a ZnSe plate. The conversion of the precursor polymer into PPV was carried out with heat treatment under dynamic vacuum.

The experimental setup for the *in situ* FTIR-ATR technique has been described in earlier papers[5-7]. Schematically, it consists of a trapezoid shaped germanium reflection element coated with a PPV film, which acts as the working electrode in the spectroelectrochemical cell (Fig. 1).

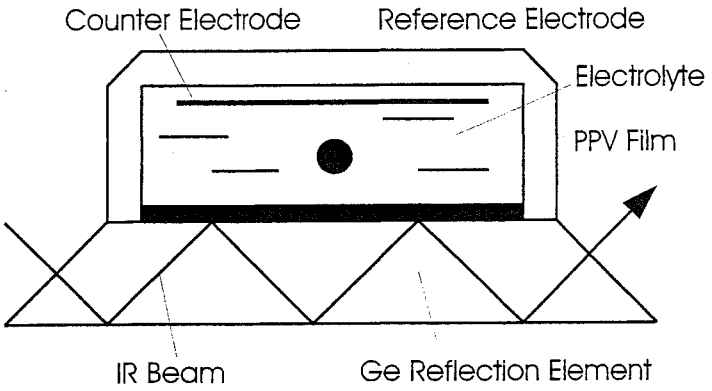


**Figure 1**: Setup for the *in situ* FTIR-ATR technique.

The electrolyte compartment of the spectroelectrochemical cell contains also a platinum foil counter electrode and a saturated calomel (SCE) reference electrode. All potential values in the paper are related to the SCE electrode potential. The electrolyte used was a 0.1 M solution of tetrabutylammoniumhexafluorophosphate ($TBAPF_6$) in acetonitrile. The spectroelectrochemical experiments were performed at room temperature. Infrared spectra were recorded consecutively during slow potential sweep experiments (sweep rate 2 mV/s) starting from 500 mV up to 1300 mV (Potentiostat Jaissle 1001 TNC, sweep generator Prodis 1/14, xy-Plotter Rikadenki, FTIR spectrometer Bruker IFS 66/S, MCT-detector, spectral resolution 4 $cm^{-1}$, 64 scans for each spectrum covering a range of ca. 60 mV in the potential sweep). Due to the small penetration depth of the evanescent wave, the measurement of the spectral changes of the polymer film during an electrochemical reaction is not significantly disturbed by the infrared absorption of the electrolyte solution. By taking an infrared spectrum just before the electrochemical reaction as the reference spectrum and relating the infrared spectra during the reaction to the reference spectrum (Fig. 2), difference spectra are obtained which represent the spectral changes of the polymer film during the electrochemical conversion. The difference spectra are displayed in absorption units.

For photoinduced absorption, the PPV covered ZnSe plate was mounted in a cryostat at an angle of 45° to the IR beam and cooled to liquid nitrogen temperature. The sample was illuminated at 45° incidence with Ar laser light (488 nm, 10 $mW/cm^2$), which could be blocked periodically with a shutter. In a series of 8000 light/dark cycles infrared transmission spectra of each illumination state were coadded. The photoinduced absorption spectrum is shown as $-\Delta T/T$, i.e. the negative transmission difference light - dark divided by the transmission of the dark state.

## RESULTS AND DISCUSSION

Figure 2 shows the current/voltage curve obtained in a spectroelectrochemical experiment with a slow potential scan from 500 mV to 1300 mV. Two electrochemical oxidation regions can be seen: a first oxidation step, appearing as a shoulder in the current/voltage curve around 1000 mV ("low oxidation" region) and a second step related with further increase of the oxidation current (exceeding the upper display limit of Figure 2) at higher potential values up to 1300 mV ("high oxidation" region).

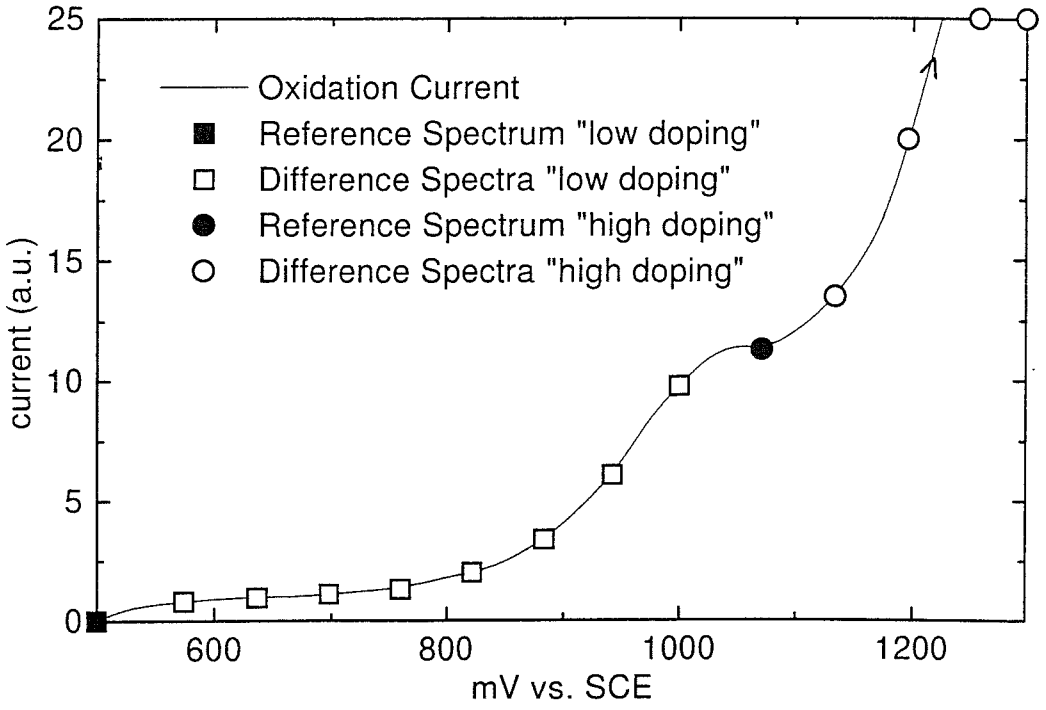


**Figure 2**: Current/voltage curve of a slow potential sweep from 500 to 1300 mV. ■ potential value of the reference spectrum for the "low oxidation" process; □ potential values for the difference spectra of the "low oxidation" process; ● potential value of the reference spectrum for the "high oxidation" process; ○ potential values for the difference spectra of the "high oxidation" process.

In Figure 3, the difference spectra obtained during the "low doping" process from 550 to 1000 mV are shown. The reference spectrum was taken at the beginning of the potential sweep at 500 mV. The most prominent feature in Fig. 3 is a broad absorption band starting around 2000 $cm^{-1}$ with a maximum higher than 5000 cm-1 (>0.6 eV). This absorption can be attributed to an electronic transition from the valence band of the conjugated π-electronic structure into a new electronic state in the band gap (polaronic or bipolaronic state)[2]. Figure 4 shows schematically the band structure of doped PPV (assuming a polaronic structure), with the electronic transition responsible for the broad absorption.

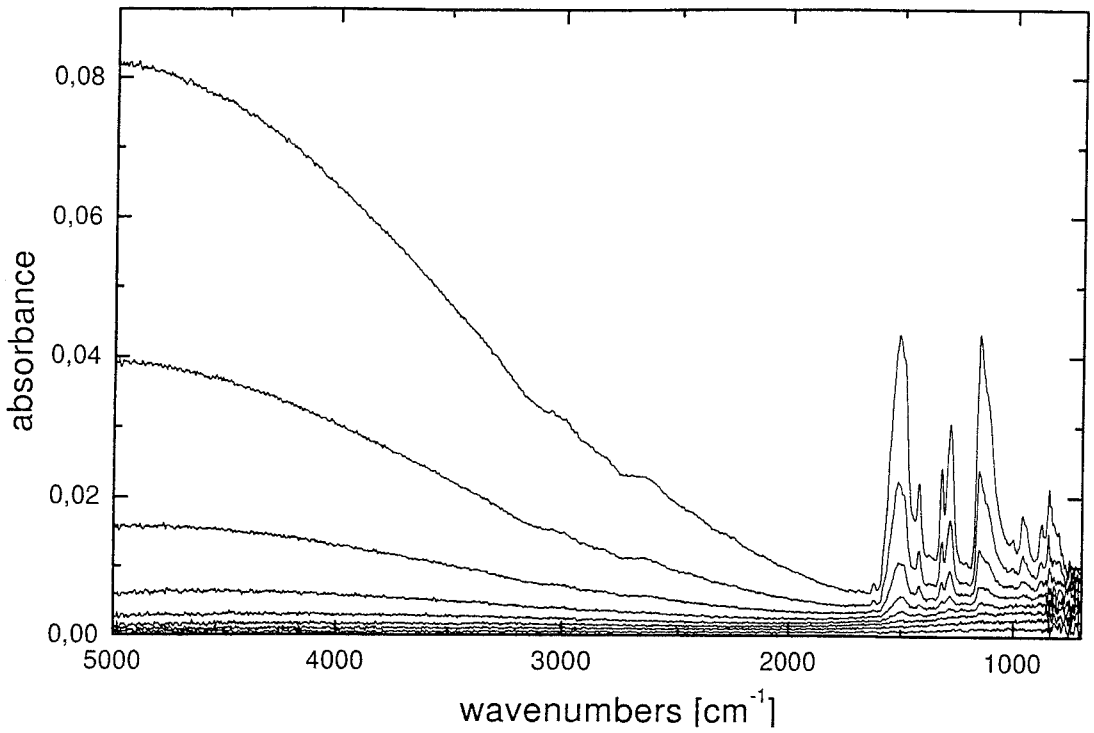


**Figure 3**: Difference spectra in the "low doping" region up to 1000 mV; reference spectrum at 500 mV.

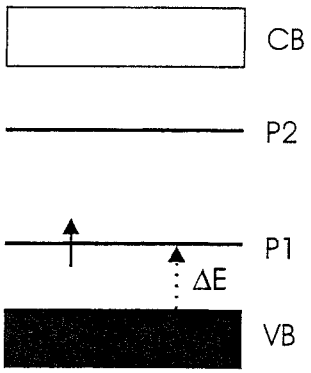


**Figure 4**: Schematic band structure of doped PPV. VB valence band, CB conduction band, P1 lower polaron band, P2 upper polaron band, ΔE electronic transition

In addition to the electronic absorption, strongly enhanced absorption bands (IRAV bands) appear in the vibrational part of the spectrum below 1700 $cm^{-1}$ (Fig. 5). The absorption maxima of the strongest bands are found at 1510, 1417, 1319, 1282 and 1153 $cm^{-1}$. The position of the bands coincide with data published in the literature obtained by chemical doping of PPV[16]. The absorption band at 844 $cm^{-1}$ originates from $PF_6^-$ anions from the $TBAPF_6$ containing electrolyte, which are incorporated into the polymer film during the oxidation reaction.

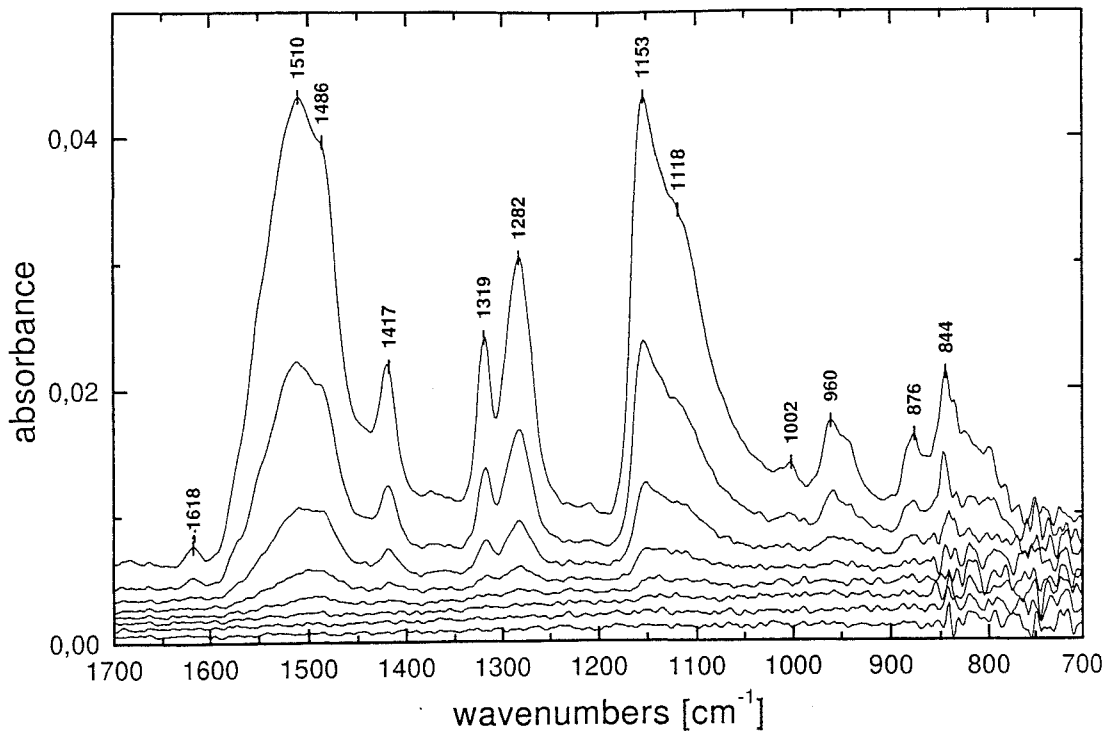


**Figure 5**: Vibrational region of Fig. 3 in an enlarged scale.

Figure 6 shows difference spectra obtained in the "high doping" region of the potential scan. The reference spectrum was taken at the end of the "low doping" process at 1060 mV. Again, a broad electronic absorption at higher energies is the most prominent feature in Fig. 6. In contrast to the band of the "low doping" process (Fig. 3), the absorption maximum is found at 4000 $cm^{-1}$ (0.5 eV). The vibrational part of the difference spectra is shown in Fig. 7. The absorption maxima of the highest IRAV bands in the "high doping" region can be seen at 1483, 1422, 1321, 1270 and 1116 $cm^{-1}$. As in the "low doping" region, the band at 844 $cm^{-1}$ correlates with the incorporation of $PF_6^-$ anions into the polymer.

Comparing the spectroelectrochemical results of the "high doping" process with the "low doping" process, the following effects occur:

- The absorption intensities of the electronic absorption as well as the IRAV bands are much higher.
- The maximum of the electronic absorption appears at lower energies (0.5 eV compared with >0.6 eV)
- The maxima of the two highest IRAV modes are found at lower wavenumbers ("low doping": 1510 $cm^{-1}$, "high doping": 1483 $cm^{-1}$; "low doping": 1153 $cm^{-1}$, "high doping": 1116 $cm^{-1}$).
- The maximum of the band at 1282 $cm^{-1}$ ("low doping") has a smaller change to 1270 $cm^{-1}$ ("high doping").
- The maxima of the bands at 1417 and 1319 $cm^{-1}$ ("low doping") are nearly unaffected (1422 and 1321 $cm^{-1}$ in the "high doping" process), taking the experimental spectral resolution of 4 $cm^{-1}$ into consideration.

Analyzing the spectral differences between the "low doping" and the "high doping" region in more detail, the maxima of the two highest IRAV modes do not show a shift, but rather an interplay of two distinct bands for each mode. In Figure 8, the maximum changes of the "low doping" and the "high doping" region in the range between 1190 and 1050 $cm^{-1}$ are compared (the spectra are scaled separately). The peak maximum at 1153 $cm^{-1}$ in the "low doping" region appears as a shoulder in the "high doping" region, whereas a shoulder at 1116 $cm^{-1}$ in the "low doping" region grows to a maximum in the "high doping" region. In a similar way, in the spectral range between 1590 and 1440 cm-1 (Fig.9) an analogous shoulder - maximum development can be seen at 1510 and 1483 $cm^{-1}$ (the shoulder in the "high doping" region appears somehow shifted). The origin of this interplay is still unknown at present time.

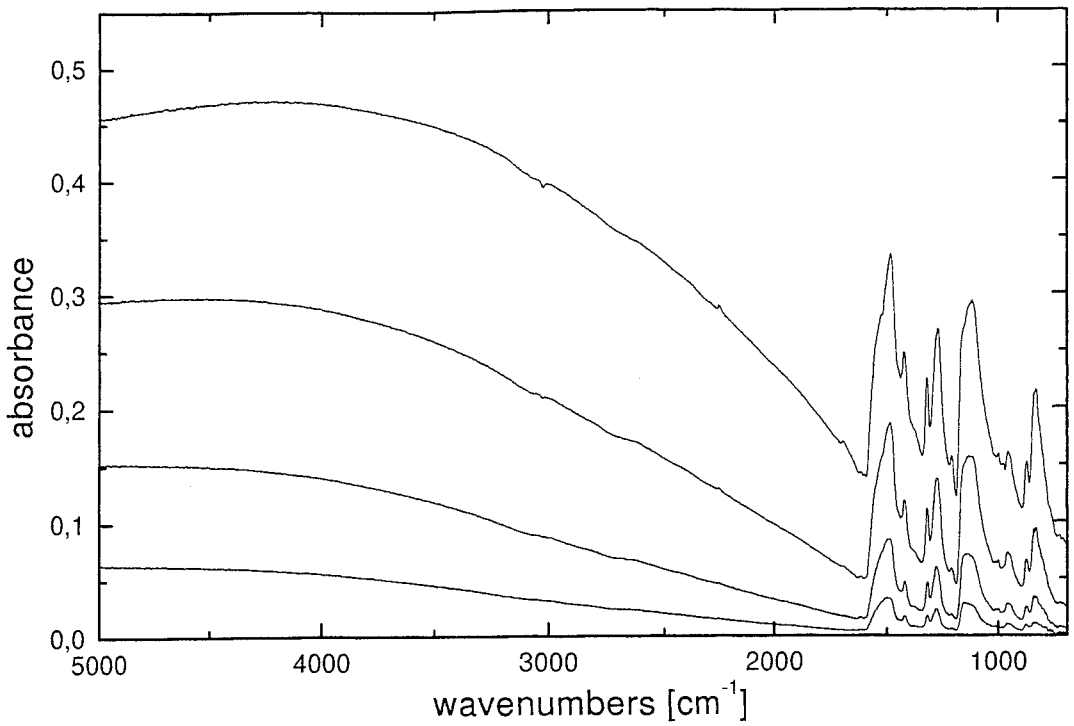


**Figure 6**: Difference spectra in the "high doping" region from 1130 to 1300 mV; reference spectrum at 1060 mV.

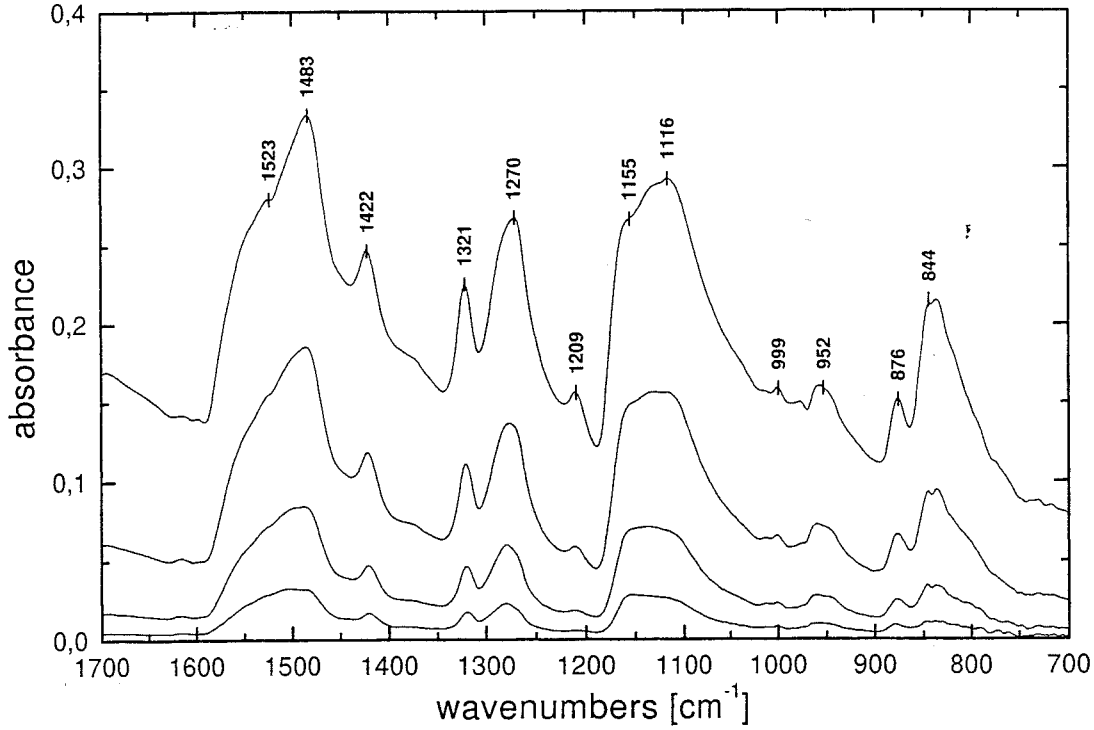


**Figure 7**: Vibrational region of Fig. 6 in an enlarged scale.

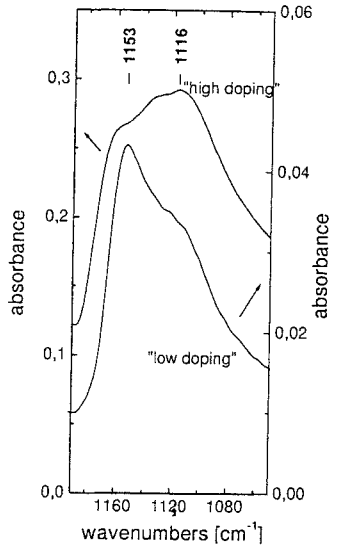


**Figure 8**: Comparison of "low doping" and "high doping" IRAV bands between 1190 and 1050 $cm^{-1}$

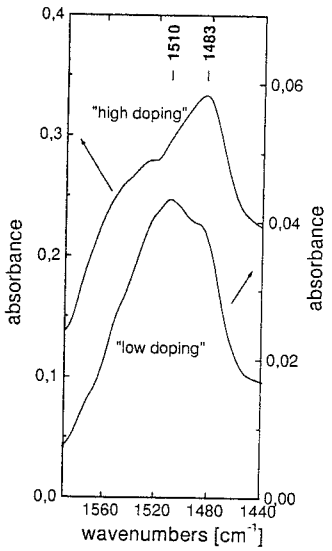


**Figure 9**: Comparison of "low doping" and "high doping" IRAV bands between 1590 and 1440 $cm^{-1}$

In Figure 10, the photoinduced absorption spectrum of a PPV film on a ZnSe substrate is shown. Similar to the electrochemically doping induced absorption (Figs. 3 and 6), the spectrum is dominated by a broad electronic absorption. The maximum of the absorption, however, is found at 3500 $cm^{-1}$ (0.45 eV). In the vibrational part of the photoinduced spectrum (Fig. 11), the main photoinduced absorption bands occur at 1479, 1411, 1313, 1274 and around 1103 $cm^{-1}$.

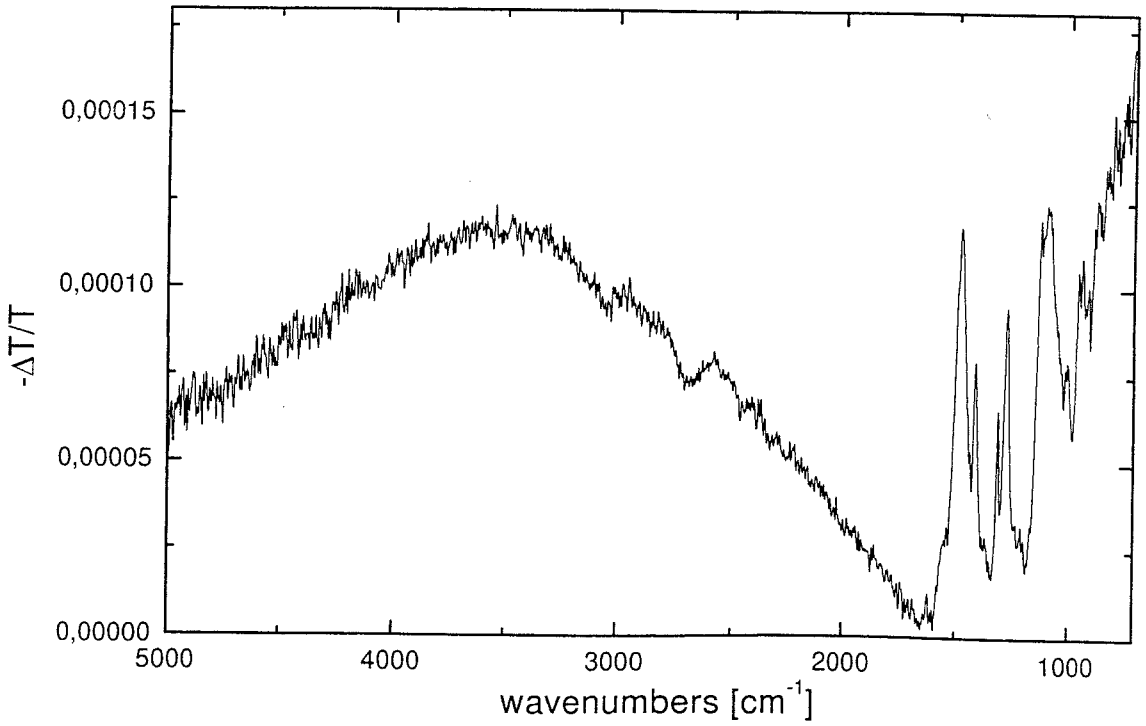


**Figure 10**: Photoinduced absorption spectrum.

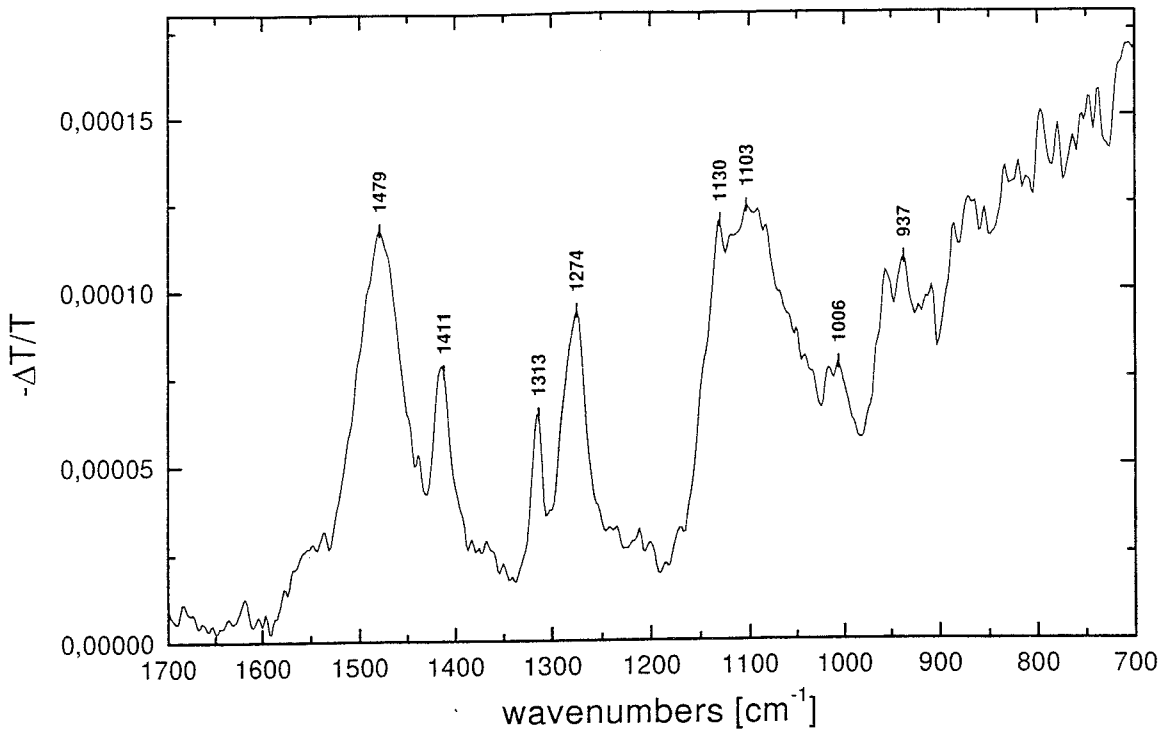


**Figure 11**: Vibrational region of Fig. 10 in an enlarged scale.

The absorption band pattern coincides with data published in the literature[16]. Table 1 shows a comparison of resonance Raman spectroscopy (RRS) data taken from the literature[17], electrochemically- and photoinduced absorption bands. For the main vibrational bands (between 1550 and 1479 $cm^{-1}$, and between 1174 and 1103 $cm^{-1}$), a decrease of the peak frequencies in the sequence RRS, "low doping", "high doping" and photoinduced absorption is found. The smaller bands (between 1422 and 1411 $cm^{-1}$, between 1335 and 1313 $cm^{-1}$, and between 1304 and 1270 $cm^{-1}$) show less changes. The frequency of the electronic absorption maximum (between >5000 $cm^{-1}$ and 3500 $cm^{-1}$) decreases from "low doping" to "high doping" and further to photoinduced absorption.

| RRS [$cm^{-1}$][17] | "low doping" [$cm^{-1}$] | "high doping" [$cm^{-1}$] | photoinduced [$cm^{-1}$] |
|---|---|---|---|
| | >5000<br>(>0.6 eV) | ~4000<br>(~0.5 eV) | ~3500<br>(~0.45 eV) |
| 1550 | 1510 | 1483 | 1479 |
| | 1417 | 1422 | 1411 |
| 1335 | 1319 | 1321 | 1313 |
| 1304 | 1282 | 1270 | 1274 |
| 1174 | 1153 | 1116 | 1103 |

**Table 1**: Comparison of RRS, doping- and photoinduced bands

Frequencies and intensities of electrochemically induced and photoinduced IRAV bands in conjugated polymers can be described with the effective conjugation coordinate (ECC) theory[3] or with the phase mode theory[4]. In the ECC theory, the spectral effects are associated with an effective conjugation force constant $f_я$, which is a measure of the effective conjugation length. In the phase mode theory, a pinning parameter $\alpha$ related to the pinning of charge density on the polymer chain (arising from dopant ions or impurities) describes the spectral behavior.

Our spectroelectrochemical experiments show, that the electrochemical oxidation process of PPV occurs in two steps, which have a different behavior regarding the position and intensities of IRAV bands and electronic absorptions. During the first step an absorption pattern similar to chemical doping experiments evolves, whereas during the second step a different absorption pattern is found (showing a higher similarity to the photoinduced infrared absorption). In the frame of the theoretical models describing frequencies and intensities of IRAV bands, the conversion of PPV from the "low doping" region into the "high doping" region during electrochemical oxidation leads to a decrease in the effective conjugation force constant $f_я$ (and a higher conjugation length) in the ECC theory or to a lower pinning parameter $\alpha$ in the phase mode theory. In accordance to the lowering of the pinning parameter, the electronic absorption moves to lower energies ($\Delta E$ in Fig 4)[18]. For the photoinduced experiment, the observed $\Delta E$ is even lower compared to doping experiments. Recently, the correlation of the IRAV frequencies with the energy of the electronic transition between valence band and the lower intergap state has been described in a theoretical model[19]. The spectral differences between the two potential regions in the spectroelectrochemical experiments can be explained by a conversion of localized charge carriers in the "low doping" region into charge carriers, which are metallicaly correlated in the "high doping" region. Further experiments are needed in order to correlate these observations quantitatively with the theoretical models and to understand the physics of the "low doping" and the "high doping" region in PPV.

## ACKNOWLEDGEMENTS

S. Srinivasan thanks the Austrian Academic Exchange Service (ÖAD) for providing a scholarship.

## REFERENCES

1. M. Zagórska, A. Pron, and S. Lefrant, *Handbook of Organic Conductive Molecules and Polymers: Vol. 3*, Chapter 4, H. S. Nalwa (ed.), John Wiley & Sons Ltd., Chichester, 1997
2. A. J. Heeger, S. Kivelson, J. R. Schrieffer, and W.-P. Su, *Rev. Mod. Phys.* **60**, pp. 781-850, 1988
3. B. Tian, G. Zerbi, and K. Müllen, *J. Chem. Phys.* **95**, pp.3198-3207, 1991
4. E. Ehrenfreund, Z. Vardeny, O. Brafman, and B. Horovitz, Phys. Rev. B 36, pp. 1535-1553, 1987
5. H. Neugebauer, *Macromol. Symp.* **94**, pp. 61-73, 1995
6. Zhao Ping, H. Neugebauer and A. Neckel, *Electrochimica Acta* **41**, pp. 767-772, 1996
7. H. Neugebauer and Zhao Ping, *Microchimica Acta*, **[Suppl] 14**, pp. 125-131, 1997
8. C. Kvarnström and A. Ivaska, *Handbook of Organic Conductive Molecules and Polymers: Vol. 4*, Chapter 9, H. S. Nalwa (ed.), John Wiley & Sons Ltd., Chichester, 1997
9. K. D. Gourley, C. P. Lillya, J. R. Reynolds, and J. C. W. Chien, *Macromolecules* **17**, pp. 1025, 1984
10. D. R. Gagnon, F. E. Karasz, E. L. Thomas, and R. W. Lenz, *Synth. Met.* **20**, pp. 85, 1987
11. I. Murase, T. Ohnishi, T. Noguchi, and M. Hirooka, *Polym. Commun.* **25**, pp. 327, 1984
12. D. R. Gagnon, J. D. Capistran, F. E. Karasz, and R. W. Lenz, *Polym. Bull.* **12**, pp. 293, 1984
13. H. Eckhardt, L. W. Shacklette, K. Y. Jen, and R. L. Elsenbaumer, *J. Chem. Phys.* **91**, pp. 1303-1315, 1989
14. J. Obrzut and F. E. Karasz, *J. Chem. Phys.* **87**, pp. 6178-6184, 1987
15. M. Herold, J. Gmeiner, W. Rieß, and M. Schwoerer, *Synth. Met.* **76**, pp. 109-112, 1996
16. K. F. Voss, C. M. Foster, L. Smilowitz, D. Mihailović, S. Askari, G. Srdanov, Z. Ni, S. Shi, A. J. Heeger, and F. Wudl, Phys. Rev. B **43**, pp. 5109-5118, 1991
17. S. Lefrant, E. Perrin, J. P. Buisson, H. Eckhardt, and C. C. Han, *Synth. Met.* **29**, pp. E91-E96, 1989
18. J.-M. André, J. Delhalle, and J.-L. Brédas, *Quantum Chemistry Aided Design of Organic Polymers*, p. 230, World Scientific Publishing Co. Pte. Ltd., Singapore, 1991
19. E. Ehrenfreund, private communication